


ARTICLE

<https://doi.org/10.1038/s42004-019-0163-y>

OPEN

Towards a light driven molecular assembler

Hanno Sell¹, Anika Gehl¹, Daniel Plaul¹, Frank D. Sönnichsen¹, Christian Schütt¹, Felix Köhler¹, Kim Steinborn¹ & Rainer Herges ¹

Chemists usually synthesize molecules using stochastic bond-forming collisions of the reactant molecules in solution. Nature follows a different strategy in biochemical synthesis. The majority of biochemical reactions are driven by machine-type protein complexes that bind and position the reactive molecules for selective transformations. Artificial “molecular assemblers” performing “mechanosynthesis” have been proposed as a new paradigm in chemistry and nanofabrication. Here we present a simple non-proteinogenic machine-type molecule which drives the endergonic condensation of vanadate to cyclic tetravanadate using light as the energy source. The system combines selective binding of the reactants, accurate positioning, and active release of the product. Hydrolysis of the product prevents inhibition of further cycles. Our prototypic system demonstrates the prerequisites that are needed to selectively drive an endergonic reaction using an external energy source.

¹Institute for Organic Chemistry, University Kiel, Otto-Hahn Platz 4, 24098 Kiel, Germany. Correspondence and requests for materials should be addressed to R.H. (email: rherges@oc.uni-kiel.de)

Most chemical processes in living organisms, unlike the larger part of synthetic chemistry, operate far from thermodynamic equilibrium¹. Major advances in synthetic and supramolecular chemistry notwithstanding^{2–5}, the control of artificial non-equilibrium systems is still in its infancy, and has been identified as a major challenge in chemistry⁶. To achieve control of such systems, a number of prerequisites have to be met that go beyond selective recognition and catalysis. A crucial point is to couple an exergonic process (driving reaction) to an endergonic reaction (driven reaction) in space and time to achieve an overall spontaneous process.

Here we demonstrate that a strong binding of the product in a ligand can drive an endergonic condensation (Fig. 1). Photochemical switching of the ligand to a non-binding state triggers the release of the product. Subsequent hydrolysis in solution allows for repeated cycles without product inhibition. While the system operates at thermodynamic equilibrium, it may serve as a prototype for the future development of biomimetic systems.

Results

Vanadate condensation equilibria. For the rational design of our prototype system, the synthesis of ATP from ADP and phosphate and the non-ribosomal peptide synthetases served as paragons. We chose the endergonic condensation of monovanadate to cyclic tetravanadate ($4 \text{HVO}_4^{2-} + 4\text{H}^+ \rightarrow \text{V}_4\text{O}_{12}^{4-} + 4 \text{H}_2\text{O}$) as the model reaction to be driven. As compared to the phosphate condensation, which would be closer to the ATP synthesis⁷, vanadate aggregation has the advantage of having a lower barrier of activation and therefore is easier to catalyze. Moreover, vanadium is one of the most NMR-sensitive nuclei in the periodic table⁸. Different vanadate aggregates give rise to distinct signals in the ⁵¹V-NMR spectrum, which can be unambiguously assigned, and whose concentrations thus can be easily determined by integration⁹. Their relative concentration depends on concentration, pH, and ionic strength of the solution (Fig. 2, for details see Supplementary Table 1, Supplementary Note 1, Supplementary Figs. 3 and 4)^{10,11}.

At pH 9.5, and a total vanadate concentration of 1.5 mM, monovanadate HVO_4^{2-} is the predominant species in solution (>95%) (Fig. 2). This monovanadate solution served as the

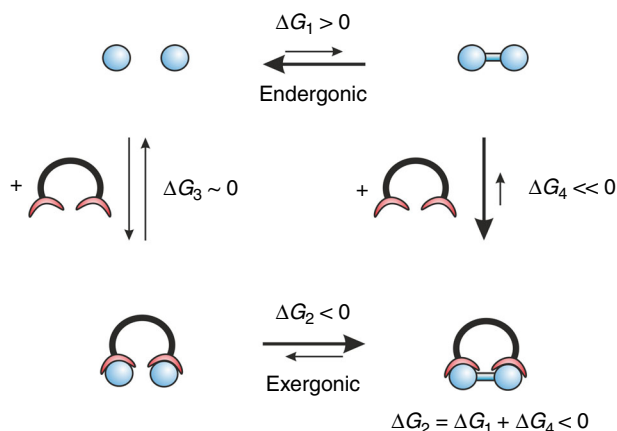


Fig. 1 Thermodynamic cycle of a dimerization model reaction, driven by strong binding of the product in a host ligand. The overall reaction is spontaneous, if the sum of the (positive) free energy of dimerization ΔG_1 is more than outmatched by the (negative) free energy of binding ΔG_4 . The dimerization reaction may either take place inside the ligand or the ligand traps small amounts of the product formed in equilibrium outside the ligand. The free energy change from the initial to the final stage is independent of the mechanism (Hess Law)

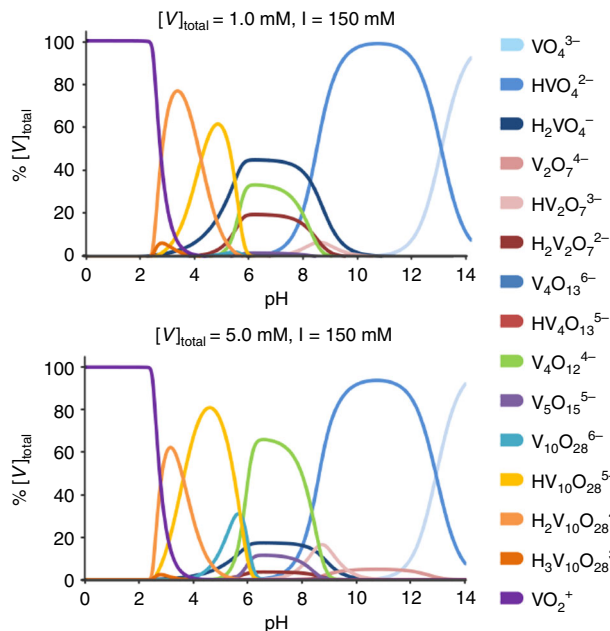


Fig. 2 Speciation of oxovanadium species as a function of pH. Percentage of different oxovanadium species in solution (speciation diagram) as a function of the pH value at an ionic strength $I = 150 \text{ mM}$. For more details see Supplementary Figs. 3 and 4, Supplementary Tables 2 and 3, Supplementary Note 1)

starting point for the design of a supramolecular system driving the endergonic tetravanadate synthesis. We chose light as the external energy source because it is convenient to apply and no interfering byproducts are formed in contrast to chemical energy sources. Moreover, vanadates are completely inert towards light of wavelengths larger than 300 nm. Therefore, no direct impact on the vanadate condensation during irradiation was expected.

Design and synthesis of the photoswitchable ligand. To couple light energy to our photochemically inert reaction, we designed a ditopic, photoswitchable receptor^{12,13}. The receptor consists of a photochromic azobenzene unit, and two Zn-cyclene moieties attached to both ends via methylene groups. Azobenzenes are very reliable, efficient, and frequently used photoswitches¹⁴, and Zn-cyclene is known to bind phosphates¹⁵ and vanadates⁹ even in water with high affinity. Upon irradiation with 365 nm light, the azobenzene isomerizes from its *trans* to the *cis* form, and light of 430 nm induces the isomerization back to the *trans* configuration. Thereby, the receptor performs a pincer-like motion ($\text{cis } \mathbf{1} \rightleftharpoons \text{trans } \mathbf{1}$, Fig. 3).

The two binding sites (Zn-cyclene units) approach each other from a distance of about 11 Å (Zn–Zn distance, open form) to less than 4 Å (closed form). Density functional theory calculations (B3LYP/6-31 G*) predict that the cyclic tetravanadate fits exactly between the two Zn-cyclen units if the ditopic receptor is in the open *trans* configuration (monovanadate and divanadate are too small and the linear trivanadate is too large, Supplementary Figs. 12 and 13 and Supplementary Note 3). A second ligand can interact with the remaining four terminal oxygen atoms, thus wrapping the tetravanadate in a tennis ball-like fashion and preventing hydrolysis. The ditopic receptor in its closed *cis* configuration does not bind any vanadate species because the two binding sites are too close to each other. Thus, upon alternating irradiation with 365 and 430 nm the ditopic receptor switches between a non-binding mode and a configuration that is strongly

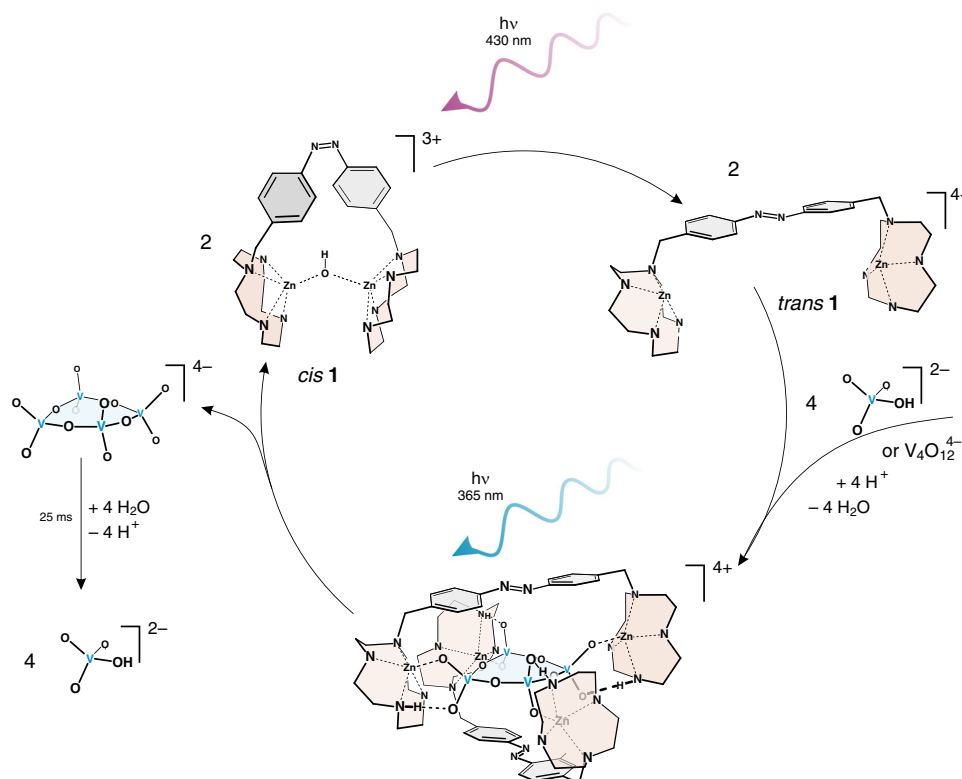


Fig. 3 Cyclic process of photoswitchable ligand **1** driving the condensation of monovanadate to cyclic tetravanadate. To enhance comprehensibility the cyclene units are shown in red, the tetravanadate ring in blue and the phenyl rings in grey shade

and selectively binding cyclic tetravanadate. The ditopic receptor was prepared in a three-step synthesis (for details see Supplementary Fig. 1)¹⁶.

Thermodynamic measurements. The monotopic ligand Zn-benzylcyclene¹² served as a reference compound. NMR titrations following the ^1H as well as the ^{51}V NMR signals reveal that there is no measurable interaction between the closed *cis*-receptor and the vanadate in solution (Supplementary Fig. 7), whereas the monotopic receptor binds vanadate with a formation constant of $\log K = 3.8$ ¹². We attribute the non-coordinating property of the ditopic *cis*-receptor to the fact that the two Zn^{2+} ions are bridged with water¹⁷, which blocks coordination with vanadate, whereas the Zn^{2+} ions are accessible in the monotopic reference compound¹². Upon titration of a monovanadate solution with the *trans*-receptor the ^{51}V NMR signal of the monovanadate decreases and the signal of the bound cyclic tetravanadate (-575 ppm) appears. After addition of 0.7 equivalents of the *trans*-ligand the ^{51}V NMR almost exclusively exhibits the tetravanadate signal (Supplementary Fig. 5). At this point 60% of the vanadate species in solution is bound as cyclic tetravanadate $\text{V}_4\text{O}_{12}^{4-}$ (Supplementary Fig. 6). At very high concentrations divanadate is formed, which is in agreement with titration experiments with the monotopic reference compound¹². To confirm the stoichiometry and to determine the stability of tetravanadate complex, the nonlinear sum of least square methods was applied to the ^{51}V NMR data^{18–21} (Supplementary Tables 2 and 3, Supplementary Figs. 5–11 and Supplementary Note 2). The data confirm the 1:2 tetravanadate to ligand stoichiometry with a very large cumulative association constant of $\log \beta = 114.2$ (Supplementary Table 3). The Gibbs free energy of complex formation (ΔG) from four molecules of protonated monovanadate (HVO_4^{2-}) and two azobenzene ligands under our experimental

conditions is $-68.3 \text{ kcal mol}^{-1}$. Proton NMR spectra are also in agreement with the theoretically predicted binding mode. Whereas the ^1H NMR spectrum of the closed form of the receptor does not change upon addition of vanadate, the phenyl proton signals of the open form broaden, and shift upfield by 0.3 ppm by anion–aromatic interactions²². The experimental value is in very good agreement with the calculated (GIAO B3LYP/6-31 G*) upfield shift of 0.4 ppm in the tennis ball-type complex compared to the free receptor (Supplementary Fig. 11). The signal broadening is due to the restriction of the conformational flexibility of the phenyl groups in the rigid complex.

The product is now stuck in the receptor and the situation corresponds to what Smalley coined the sticky finger problem²³. However, upon irradiation with UV light (365 nm), the ligands can be converted to the non-binding *cis* configuration and the product is released. The free cyclic tetravanadate is not stable outside of the receptor under our experimental conditions (pH 9.53). It hydrolyses back to monovanadate with a half-life of 25 ms²⁴. The switching of the vanadate aggregation states is impressively demonstrated by a ^{51}V NMR experiment. Switching experiments were performed by alternating irradiation with 365 and 440 nm (Fig. 4). In the closed form of the receptor monovanadate is the predominant vanadate species in solution (83%). The small amount of tetravanadate (17%) can be attributed to incomplete conversion to the *cis* isomer in the photostationary equilibrium. Irradiation with 440 nm leads to the open form of the receptor accompanied by the condensation of the monovanadate to tetravanadate. Twenty-five percent of the monovanadate is transformed into tetravanadate. Subsequent closing of the receptor molecule through *trans*-*cis* isomerization results in the release of the tetravanadate, which hydrolyses instantly to monovanadate. The switching can be repeated for a large number of cycles without fatigue (Supplementary Note 4 and Supplementary Fig. 14).

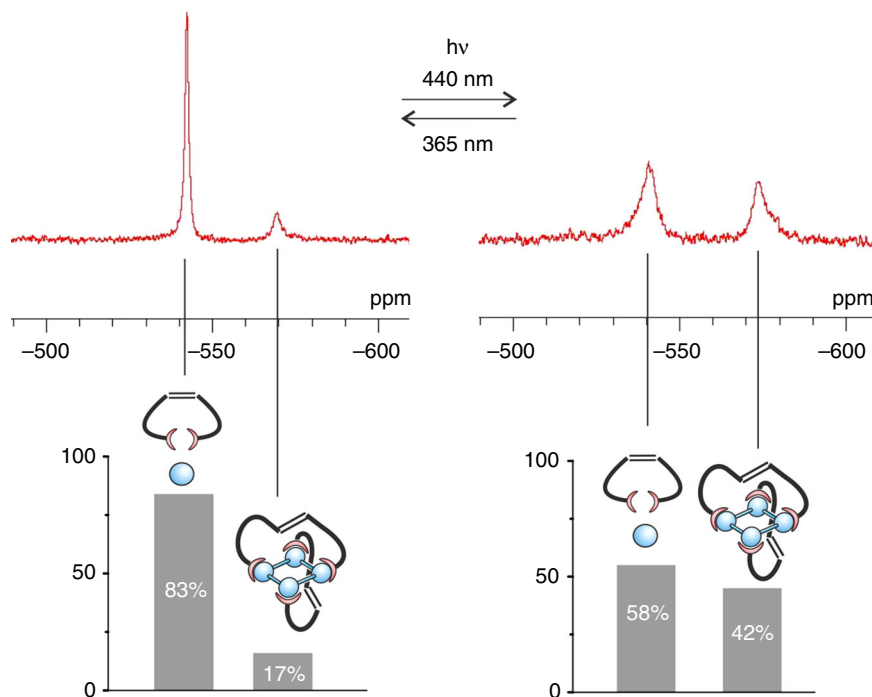


Fig. 4 Photoswitching of vanadate aggregation. ^{51}V -NMR spectra of the two photostationary states of a vanadate/ligand solution (1.5 mM Na_3VO_4 , 100 mM CHES buffer, 50 mM NaOH, pH 9.53, $I = 150$ mW, 0.75 mM receptor) upon irradiation **a** with 365 nm and **b** 440 nm. The structural schemes (for explanation see Fig. 5) represent the vanadate/ligand species that contribute to the corresponding ^{51}V NMR signals above, and the bars indicate the relative concentrations. The incomplete photochemical conversion of the ligand from the *trans* to the *cis* isomer (70%) accounts for the 17% tetravanadate in solution (**a**). Upon heating to 70 °C for 30 min conversion is complete and the tetravanadate signal is reduced below the detection limit (Supplementary Fig. 5)

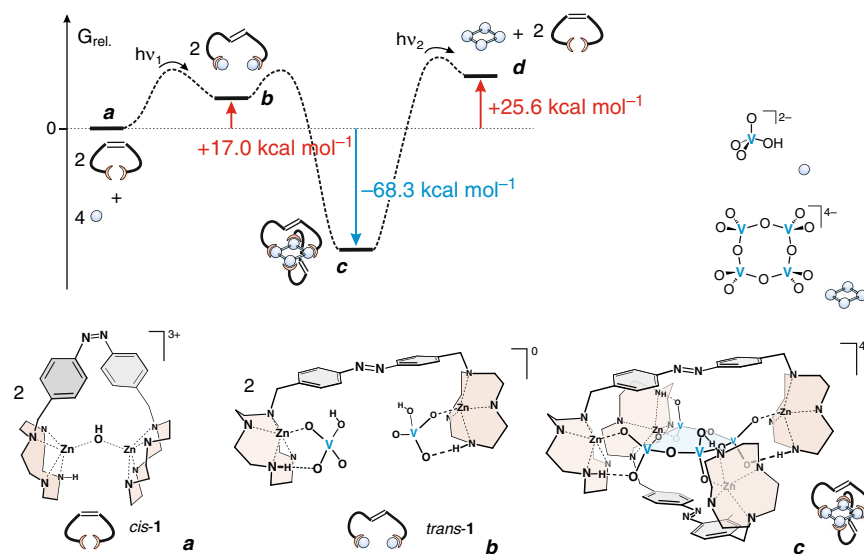


Fig. 5 Gibbs free energy hypersurface of the ligand-driven vanadate condensation. The G values refer to the experimentally used amounts and concentrations of *cis* ligand, monovanadate, and buffer at pH 9.53. Sample volume: 500 μL , Na_3VO_4 : 1.5 mM, ligand: 1.05 mM, CHES buffer: 100 mM, NaOH: 50 mM, I : 150 mW. The different stages of the reaction path are labeled with **a**, **b**, **c**, and **d**. The system is assumed to be in equilibrium in all stages

From the ^{51}V NMR titration data of the monotopic reference ligand⁹, and the ditopic ligand, the Gibbs free energy (ΔG_{rel}) of four stages of the condensation reaction was determined (for details see Supplementary Table 5 and Supplementary Note 6). Note that the values do not include the energies of the ligand in *cis* and *trans* configuration, and are calculated based on the experimental conditions (see Fig. 5) to avoid ambiguities²⁵. Binding of two monovanadate molecules to the ditopic ligand is

slightly endergonic at our reaction conditions (values determined from the monotopic ligand⁹ assuming that there is no interaction between the two binding sites, which are ~ 11 Å apart). The condensation reaction forming the cyclic tetravanadate in the presence of the ligand is strongly exergonic ($-68.3 \text{ kcal mol}^{-1}$, stage **c**, Fig. 5), whereas it is endergonic without ligand in solution ($+25.6 \text{ kcal mol}^{-1}$, stage **d**). The 2:1 complex (stage **c**) is the lowest point on the Gibbs free energy surface. Without

further energy input the reaction would stop at this point and the ligand would not be available for further cycles (Fig. 3). Two equivalents of the ligand could only generate one equivalent of the product. A continuously operating assembler, however, has to operate many cycles without fatigue to justify the effort of its synthesis. In our case, active release of the product is achieved by photochemical switching of the ligand to the non-binding *cis* isomer. We would like to emphasize that this photochemically driven release of the product is the most energy-consuming process of the condensation cycle (in analogy to ATP synthase)²⁶. Outside the ligand the cyclic tetravanadate is kinetically unstable and spontaneously hydrolyses back to monovanadate ($t_{1/2} = 25$ ms)²⁰. By switching of the ligand back to the *trans* isomer (440 nm) the next assembly cycle is started. Photoswitching experiments (irradiation with 365 and 440 nm in an alternating sequence) prove that our system performs a large number of cycles without detectable fatigue (Supplementary Note 4, Supplementary Fig. 14).

Discussion

In conclusion, we have presented a prototype light-driven, molecular machine-type ligand, which mediates the endergonic condensation of monovanadate to cyclic tetravanadate. By positioning the reactants, the photoswitchable ligand guides the reactants through a specific reaction channel, and a molecule is formed that is not present in the starting solution, and which would not form spontaneously. Upon switching of the ligand to a non-binding state, the high energy cyclic tetravanadate is released and hydrolyses to monovanadate. The system does not exhibit measurable fatigue over a large number of cycles. Light energy is converted to chemical energy, similar to the formation of ATP from ADP and phosphate. Mechanosynthesis with artificial molecular assemblers is extremely challenging but worthwhile investigating. Developed up to the level of biochemical systems such as non-ribosomal peptide synthetases, and polyketide synthases, it would allow chemo-, regio-, and stereoselective synthesis without protecting groups or chiral auxiliaries, and has the potential to become an alternative paradigm in chemical synthesis. Moreover, molecular assemblers provide an alternative way of converting light into chemical energy.

Methods

Experimental procedures. See Supplementary Figs. 1 and 2 and Supplementary Methods.

Vanadate equilibria in solution as a function of pH and ionic strength. See Supplementary Table 1, Supplementary Figs. 3 and 4 and Supplementary Note 1.

NMR titrations. See Supplementary Tables 2 and 3, Supplementary Figs. 5–11 and Supplementary Note 2.

Theoretical calculations. See Supplementary Figs. 12, 13, Supplementary Table 4, and Supplementary Note 3.

Photoswitching experiments. See Supplementary Fig. 14 and Supplementary Note 4.

Calculation of relative free energies. See Supplementary Table 5 and Supplementary Note 5.

Estimation of the light to chemical energy efficiency. See Supplementary Note 6.

Data availability

The data that support the plots within this paper and other findings of this study are available from the corresponding authors upon reasonable request.

Received: 2 February 2019 Accepted: 16 May 2019

Published online: 07 June 2019

References

1. Fischbach, M. A. & Walsh, C. T. Assembly-line enzymology for polyketide and nonribosomal peptide antibiotics: logic, machinery, and mechanisms. *Chem. Rev.* **106**, 3468–3496 (2006).
2. Meng, W. et al. An autonomous molecular assembler for programmable chemical synthesis. *Nat. Chem.* **8**, 542–548 (2016).
3. Kassem, S. et al. Stereodivergent synthesis with a programmable molecular machine. *Nature* **549**, 374–378 (2017).
4. De, Bo, G. et al. An artificial molecular machine that builds an asymmetric catalyst. *Nat. Nanotech.* **13**, 381–385 (2018).
5. Lewandowski, B. et al. Sequence-specific peptide synthesis by an artificial small-molecule machine. *Science* **339**, 189–193 (2013).
6. Coskun, A., Banaszak, M., Astumian, R. D., Stoddart, J. F. & Grzybowski, B. A. Great expectations: can artificial molecular machines deliver on their promise? *Chem. Soc. Rev.* **41**, 19–30 (2012).
7. Hosseini, M. W. & Lehn, J.-M., Supramolecular catalysis: substrate phosphorylations and adenosine triphosphate synthesis with acetylphosphate catalysed by a macrocycle polyamine. *Chem. Commun.* 397–399 (1988).
8. Pregosin, P. S. *Transition Metal Nuclear Magnetic Resonance* (Elsevier, Amsterdam 1991).
9. Crans, D. C., Shin, P. K. & Armstrong, K. B. Application of NMR spectroscopy to studies of aqueous coordination chemistry of vanadium (V) complexes. *Adv. Chem.* **246**, 303–318 (1995).
10. Pettersson, L., Hedman, B., Andersson, I. & Ingri, N. Multicomponent polyanions. 34. A potentiometric and ^{51}V NMR study of equilibria in the $\text{H}^+ - \text{HVO}_4^{2-}$ system in 0.6 M NaCl medium. *Chem. Scr.* **22**, 254–264 (1983).
11. Pettersson, L., Andersson, I. & Hedman, B. Multicomponent polyanions. 37. A potentiometric and ^{51}V NMR study of equilibria in the $\text{H}^+ - \text{HVO}_4^{2-}$ system in 3.0 M sodium perchlorate medium. *Chem. Scr.* **25**, 309–317 (1985).
12. Sell, H., Gehl, A., Sönnichsen, F. D. & Herges, R. Thermodynamic and kinetic stabilization of divanadate in the monovanadate/divanadate equilibrium using a Zn-cyclene derivative: towards a simple ATP synthase model. *Beilstein J. Org. Chem.* **8**, 81–89 (2012).
13. Zhang, X. & Woggon, W.-D. A supramolecular fluorescence sensor for pyrovanadate as a functional model of vanadium haloperoxidase. *J. Am. Chem. Soc.* **127**, 14138–14139 (2005).
14. Bandara, H. M. D. & Burdette, S. C. Photoisomerization in different classes of azobenzene. *Chem. Soc. Rev.* **41**, 1809–1825 (2012).
15. Kimura, E., Aoki, S., Koike, T. & Shiro, M. A tris(ZnII -1,4,7,10-tetraazacyclododecane) complex as a new receptor for phosphate dianions in aqueous solution. *J. Am. Chem. Soc.* **119**, 3068–3076 (1997).
16. Maie, K., Mitsunobu, N. & Kazushige, Y. Conformational changes of DNA by photoradiation of DNA-bis(ZnII -cyclen)-azobenzene complex. *Nucleosides Nucleotides Nucleic Acids* **25**, 435–462 (2006).
17. Xiang, Q.-X. et al. Dinuclear macrocyclic polyamine zinc(II) complexes: syntheses, characterization and their interaction with plasmid DNA. *J. Inorg. Biochem.* **99**, 1661–1669 (2005).
18. Cruywagen, J. Heyns, J. Vanadium(V) equilibria. Spectrophotometric and enthalpimetric investigation of the dimerization and deprotonation of HVO_4^{2-} . *Polyhedron* **10**, 249–253 (1991).
19. Ingri, N. et al. LAKE—a program system for equilibrium analytical treatment of multimethod data, especially combined potentiometric and nuclear magnetic resonance data. *Chem. Scand. Acta* **50**, 717–734 (1996).
20. Schmidt, H., Andersson, I., Rehder, D. & Pettersson, L. A potentiometric and ^{51}V NMR study of the aqueous $\text{H}^+/\text{H}_2\text{VO}_4^-/\text{H}_2\text{O}_2/\text{L}-\alpha\text{-alanine-L-histidine}$ system. *Chem. Eur. J.* **7**, 251–257 (2001).
21. Del Piero, S., Melchior, A., Polese, P., Portanova, R. & Tolazzi, M. A novel multipurpose excel tool for equilibrium speciation based on Newton–Raphson method and on a hybrid genetic algorithm. *Annali di Chimica* **96**, 29–49 (2006).
22. Schottel, B. L., Chifotides, H. T. & Dunbar, K. R. Anion π -interactions. *Chem. Soc. Rev.* **37**, 68–83 (2008).
23. Drexler, K. E. & Smalley, R. E. *Nanotechnol. CN Cover story* **81**, 37–42 (2003).
24. Crans, D. C., Rithner, C. D. & Theisen, L. A. Application of time-resolved ^{51}V 2D NMR for quantification of kinetic exchange pathways between vanadate monomer, dimer, tetramer, and pentamer. *J. Am. Chem. Soc.* **112**, 2901–2908 (1990).
25. Rosing, J. & Slater, E. C. The value of ΔG° for the hydrolysis of ATP. *Biochim. Biophys. Acta* **267**, 275–290 (1972).
26. Boyer, P. D., Cross, R. L. & Momsen, W. A new concept for energy coupling in oxidative phosphorylation, based on molecular explanation of the oxygen exchange reactions. *Proc. Natl Acad. Sci. USA* **70**, 2837–2839 (1973).

Acknowledgements

We gratefully acknowledge support by the German Research Foundation (DFG) via SFB 677.

Author contributions

A.G., H.S., D.P., and K.S. did the experiments. C.S. and F.K. performed the quantum chemical calculations. F.S. performed the NMR experiments. R.H. conceived and supervised the experiments. R. H. and H.S. wrote the manuscript.

Additional information

Supplementary information accompanies this paper at <https://doi.org/10.1038/s42004-019-0163-y>.

Competing interests: The authors declare no competing interests.

Reprints and permission information is available online at <http://npg.nature.com/reprintsandpermissions/>

Publisher's note: Springer Nature remains neutral with regard to jurisdictional claims in published maps and institutional affiliations.



Open Access This article is licensed under a Creative Commons Attribution 4.0 International License, which permits use, sharing, adaptation, distribution and reproduction in any medium or format, as long as you give appropriate credit to the original author(s) and the source, provide a link to the Creative Commons license, and indicate if changes were made. The images or other third party material in this article are included in the article's Creative Commons license, unless indicated otherwise in a credit line to the material. If material is not included in the article's Creative Commons license and your intended use is not permitted by statutory regulation or exceeds the permitted use, you will need to obtain permission directly from the copyright holder. To view a copy of this license, visit <http://creativecommons.org/licenses/by/4.0/>.

© The Author(s) 2019